



## TSUNAMI INUNDATION MODELING AND HAZARD MAPPING USING GIS IN SAWARNA BEACH, BANTEN PROVINCE

**Thema Arrisaldi<sup>1\*</sup>, Muhammad Amin Arya Bima<sup>2</sup>, Kanya Kirana Ramadhani Nurapita<sup>3</sup>, Puji Pratiknyo<sup>1</sup>**

<sup>1</sup>. Department of Geological Engineering, Faculty of Mineral and Energy Engineering,  
UPN VETERAN

Jl. Padjajaran Ring Road Utara No.104, Ngropoh, Condongcatur, Depok, Sleman,  
Special Region of Yogyakarta, 55283

<sup>2</sup> Department of Earth Science, College of Earth Science, National Central University  
No. 300, Zhongda Rd, Zhongli District, Taoyuan City, Taiwan 320

<sup>3</sup> Department of Geological Engineering, Faculty of Engineering, Gadjah Mada University  
Bulaksumur, Depok, Sleman Regency, Special Region of Yogyakarta, 55281

\*Email: [thema.arrisaldi@upnyk.ac.id](mailto:thema.arrisaldi@upnyk.ac.id)

Submitted: 25/05/2025 Revised: 30/06/2025 Accepted: 01/07/2025

### **Abstract**

*Tsunamis pose significant hazards to coastal areas, particularly in tectonically active regions like the southern coast of Java. This study models tsunami inundation at Sawarna Beach, Banten Province, using a quantitative spatial analysis approach. By integrating Digital Elevation Model (DEM) data from DEMNAS and land cover data from BIG, a tsunami hazard index is generated through slope analysis, surface roughness coefficients, and cost distance modeling within a GIS framework. The analysis reveals that areas with low surface roughness and gentle slopes are more prone to deep inland tsunami inundation. Vulnerability mapping under simulated tsunami heights (5m, 10m, 15m, and 30m) shows that hazard zones significantly increase with wave height, with the highest exposure at 30m reaching nearly 15 million m<sup>2</sup>. The study underscores the importance of accurate topographic data for disaster mitigation planning and provides essential recommendations for local stakeholders in land use and infrastructure development. These findings serve as a valuable reference for enhancing tsunami preparedness and resilience in coastal communities.*

**Keywords:** DEM, GIS, Hazard Index, Tsunami Inundation, Vulnerability Mapping

### **1. INTRODUCTION**

Tsunamis are classified as natural disasters with high-risk levels due to their potential to cause significant damage, influenced by several key factors, including strong water currents, debris carried by the waves, the potential for fire and contamination, inundation, and seawater pollution (Berryman, 2005). Tsunamis are primarily caused by sudden seafloor deformation due to subduction-zone

earthquakes, and may also result from earthquake-triggered submarine landslides, volcanic eruptions, or underwater manmade explosions (Sundar et al., 2020).

Western Indonesia is known as one of the most seismically active regions in the world due to the presence of the Sunda subduction zone, which dips northward (Koesoemadinata, 2020). McCaffrey (2008) stated that the entire subduction zone theoretically has the potential

to generate earthquakes of magnitude greater than Mw 9, including the subduction zone off the coast of Java, which is one of the longest subduction segments in the world. Seismic activity in the southern part of West Java (Fig. 1) shows the distribution of shallow earthquakes ( $\leq 70$  km) with magnitudes greater than 5 Mw over the past 20 years (USGS Earthquake Catalog, 2025). This distribution indicates that the region continues to experience significant tectonic activity.

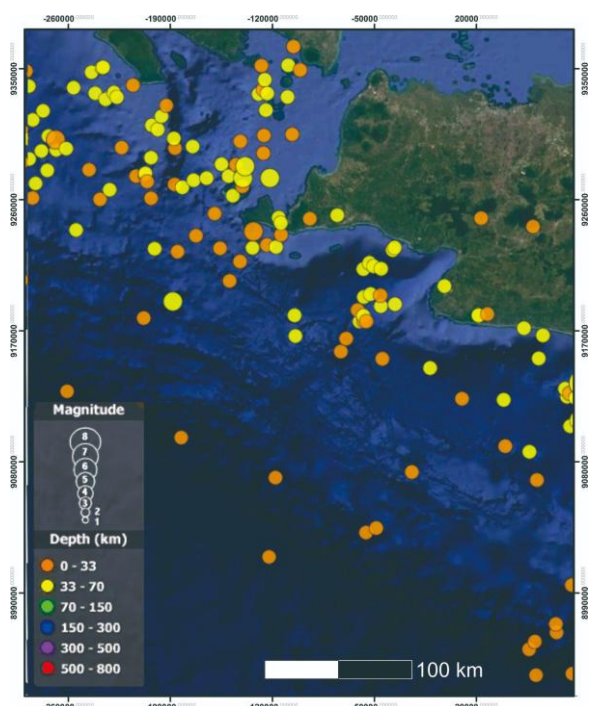


Fig. 1. Distribution of shallow earthquakes ( $\leq 70$  km) with magnitudes  $\geq 5$  Mw in the southern part of West Java over the past 20 years, based on the USGS Earthquake Catalog (2025), overlaid on a Google Earth base map. The color of the markers represents depth, and their size indicates earthquake magnitude.

The southern coast of Java Island, including Sawarna Beach in Banten Province, is considered a highly vulnerable area to tsunamis. In addition to geological factors, the presence of tourist destinations in this area increases human exposure to tsunami hazards, thereby raising the overall disaster risk potential. Based on the Indonesian Tsunami Catalog (Yudhicara et al., 2023), Java Island has experienced 22

tsunami events, with West Java recording the highest frequency (8 events). The most recent tsunami in 2006 caused 668 fatalities and inundated coastal areas up to 500 meters inland. The closest historical event to the study area was the 1915 tsunami in Cisolok, which produced 2-meter waves and an 8-meter run-up. These records highlight the persistent tsunami hazard in the region. As a coastal tourism destination, Sawarna Beach requires a business continuity plan, one of the key efforts of which is to enhance the sector's resilience to natural disasters originating from coastal hazards (Rahayu et al., 2024). According to Tonini et al. (2021), inundation maps are a fundamental tool for coastal risk management, particularly in supporting the development of evacuation maps and planning strategies to ensure effective disaster response. Geological evidence has been instrumental in estimating inland inundation distances and flow depths of recent tsunamis (Goto et al., 2011). Field surveys from the 2011 Tohoku tsunami provide detailed insight into how wave height and run-up vary inland (Mori et al., 2011). Advanced inundation modeling reveals that tsunami wave heights can remain destructive far inland under certain topographic and roughness conditions (Wei et al., 2013). Detailed modeling for Java's southern coast highlights how high-resolution bathymetry enhances inundation accuracy inland (Prasetya et al., 2021). Validated tsunami models using damage data from Sulawesi in 2018 have improved inland hazard prediction (Adriano et al., 2020). Integration of DEMNAS and land use classification in Java's coastal areas improves tsunami zoning accuracy (Putra et al., 2022). Rough terrain and vegetation significantly reduce tsunami energy as waves move inland (Gusman et al., 2023). Scenario-based simulations for Banten suggest that even moderate tsunami waves can inundate deep inland under low-slope conditions (Fitriani et al., 2024). Therefore, this study aims to model a tsunami inundation scenario in the Sawarna Beach area using a quantitative approach based

on topographic data. The results of this study are expected to serve as a foundation for communities and local governments in designing more accurate and effective disaster mitigation strategies.

## 2. METHODOLOGY

This study employs a quantitative approach using spatial analysis methods to map and analyze potential tsunami wave inundation. The research is conducted by utilizing spatial data and Geographic Information System (GIS)-based modeling through ArcGIS and QGIS software (Budiman, 2024).

The primary data used in this study include a Digital Elevation Model (DEM) obtained from DEMNAS (Geospatial Information Agency/BIG) and land cover data, also provided by BIG, accessed in May 2025. The DEM is used to determine elevation contours in coastal areas, while the land cover data help identify land use types affected by tsunami waves. The overall workflow of the tsunami hazard index estimation process is illustrated in Figure 2. It outlines the sequential steps involved, starting from data preprocessing to the final hazard index classification using a fuzzy membership approach.

The analysis consists of several stages:

- Data preprocessing:** including correction and clipping of DEM and land cover data to match the study area.
- Slope calculation:** using geoprocessing tools in ArcGIS to identify risk-prone areas based on topography.
- Conversion of slope to radians:** for mathematical calculations in the tsunami height loss model.
- Tsunami wave height loss (Hloss) per meter** is calculated using Equation 1.

$$H_{loss} = \left( \frac{167 \cdot n^2}{H_0^{1/3}} \right) + 5 \cdot \sin(S) \quad (1)$$

where:

$n$  = surface roughness coefficient (determined by land cover type)

$H_0$  = initial tsunami wave height at the shoreline

$S$  = slope (in radians)

- Spatial overlay with Cost Distance analysis:** the  $H_{loss}$  model output is used as a cost surface, where each pixel represents energy loss due to elevation and land cover differences.
- Transformation using fuzzy membership:** this method converts the cost distance values into a scale from 0 to 1, representing the relative vulnerability to tsunami inundation.
- Calculation of the affected area.** The affected area is calculated using the calculate geometry tool within the ArcGIS software (Suri, 2024).

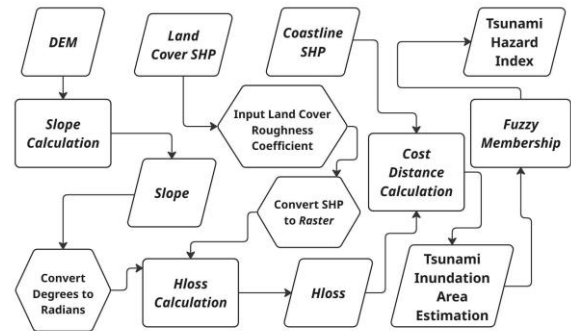


Fig. 2. Workflow for estimating the tsunami hazard index using DEM, land cover, and coastline data. The diagram illustrates the analysis steps, starting from slope calculation to the determination of the tsunami hazard index using the cost distance and fuzzy membership methods.

## 3. RESULT AND DISCUSSION

The roughness was generated based on a shapefile (SHP) that already contained roughness coefficient values, which were then converted into raster data using the Feature to Raster tool in ArcGIS. The raster resolution was adjusted to match the resolution of the DEM to produce a more detailed analysis. The most rough surface is from forest which has 0.7 coefficient and the least rough surface is the water body which has 0.007 coefficient (Table 1).

Table 1. Surface Roughness Coefficient

Land Cover Type	Surface Roughness Coefficient
<b>Water Body</b>	0.007
<b>Shrubs/Bushes</b>	0.04
<b>Forest</b>	0.07
<b>Plantation/Estate</b>	0.035
<b>Crops</b>	
<b>Bare/Open Land</b>	0.015
<b>Agricultural Land</b>	0.025
<b>Settlement/Built-up Area</b>	0.045
<b>Mangrove</b>	0.025
<b>Fishpond/Embankment</b>	0.01

(Berryman, 2005)

Table 2 presents the classification and area of each land cover type in square meters (m<sup>2</sup>). Forests constitute the most dominant land cover, with an area reaching 121,640,347.24 m<sup>2</sup>, highlighting their crucial role as the primary vegetative component in the study area. Other land cover types with significant coverage include rice fields covering 30,886,306.31 m<sup>2</sup>, plantations with 13,766,830.86 m<sup>2</sup>, and agricultural land totaling 9,982,978.03 m<sup>2</sup>. Residential or built-up areas are also substantial, amounting to 8,635,252.31 m<sup>2</sup>, reflecting land use for anthropogenic purposes. Meanwhile, land cover types with the smallest areas include fishponds (2,683.21 m<sup>2</sup>), other non-cultivated vegetation (63,453.47 m<sup>2</sup>), and inland sand dunes (30,892.44 m<sup>2</sup>). The spreading of the land cover can be seen in Fig. 4.

The slope map (Fig. 3), an essential input for inundation analysis, was generated based on DEMNAS data provided by BIG with a 0.27 arc-second resolution, which is higher than the 3 arc-second resolutions of global DEM data (Iswari & Anggraini, 2018). Higher resolution improves slope accuracy and enhances model reliability (Sarah et al., 2024).

The tsunami hazard index is influenced by parameters such as tsunami wave height, surface roughness coefficient, coastal line and slope steepness (Berryman, 2005). Tsunami run-up simulations along the southern Java coast

suggest significant inundation potential in low-slope inland zones (Tanioka et al., 2018). As mentioned, coastal areas with gentler slopes tend to have a higher likelihood of disaster. In addition, areas with lower land surface roughness coefficients are generally more vulnerable to tsunami hazards. As shown in Fig. 5, tsunami hazard-prone areas are distributed along the coastline. Coastal regions with relatively steep slopes have a narrower distribution of tsunami-prone zones.

Table 2. Land Cover Area

Land Cover Type	Area (m <sup>2</sup> )
<b>Coral Rock</b>	138,653.50
<b>Lake/Pond</b>	15,897.421
<b>Buildings</b>	8,635,252.31
<b>Forest</b>	121,640,347.24
<b>Fishpond</b>	2,683.21
<b>Inland Sand Dune/Sand Hill</b>	30,892.44
<b>Coastal Sand Dune/Sand Hill</b>	704,844.62
<b>Plantation</b>	13,766,830.86
<b>Rice Field</b>	30,886,306.31
<b>Shrub</b>	2,749,227.18
<b>River</b>	1,947,747.25
<b>Bare Land</b>	2,804,436.83
<b>Agricultural</b>	9,982,978.03
<b>Other Non-Cultivated Vegetation</b>	63,453.47

In contrast, the tsunami hazard vulnerability index expands significantly in areas with gentle slopes. Land cover also plays a crucial role. Tsunami hazard vulnerability zones extend far inland through areas classified as "water bodies," in this case, rivers. The combination of gentle slopes and low-coefficient land cover causes the zones to penetrate deeply and extensively inland.

Table 3. presents the area coverage (in square meters) based on tsunami vulnerability classes (high, medium, and low) under various simulated tsunami wave heights—5 meters, 10 meters, 15 meters, and 30 meters. The data indicate that as the tsunami wave height increases, the area categorized under high vulnerability also increases significantly. For instance, at a 5-meter wave height scenario, the high vulnerability zone covers 1,189,572.35 m<sup>2</sup>.

However, this figure increases drastically to 13,689,164.84 m<sup>2</sup> under a 30-meter wave scenario.

A similar trend is observed for the medium and low vulnerability classes, although the increase is less significant than that for the high vulnerability class. The medium vulnerability area grows from 698,306.37 m<sup>2</sup> at 5 meters to 849,884.79 m<sup>2</sup> at 30 meters. Meanwhile, the low vulnerability class increases from 382,054.34 m<sup>2</sup> to 439,723.06 m<sup>2</sup> under the same conditions.

This pattern indicates that higher tsunami wave scenarios tend to significantly expand the coverage of high-vulnerability zones while relatively reducing the proportions of medium and low-vulnerability zones. The pattern suggests larger tsunami events are more likely to significantly affect coastal areas with relatively flat slopes and low land cover roughness coefficients.

Table 3. Influenced Area During Several Height of Tsunami Wave

Vulnerability	Covered Area (m <sup>2</sup> )			
	5m	10m	15m	30m
High	1,189,572.35	3,415,214.33	5,768,376.70	13,689,164.84
Middle	698,306.37	757,906.82	786,774.34	849,884.79
Low	382,054.34	367,224.87	382,743.58	439,723.06
Total	2,269,933.05	4,540,346.02	6,937,894.62	14,978,772.69

#### 4. CONCLUSION

The total area impacted by the tsunami hazard index around Sawarna Beach varies based on wave height. For a 5-meter wave, the affected area is 2,269,933.05 m<sup>2</sup>. In the case of a 10-meter wave, the area impacted increases to 4,540,346.02 m<sup>2</sup>. A 15-meter wave scenario affects an area of 6,937,894.62 m<sup>2</sup>. The most significant impact occurs in the 30-meter wave

scenario, which affects a total area of 14,978,772.69 m<sup>2</sup>.

Coastal areas that are open, have relatively low land cover roughness, and gentle slopes (0–7°) are particularly vulnerable to inundation. This includes environments such as bodies of water, fishponds, and open land.

#### 5. RECOMMENDATION

1. Utilize Digital Elevation Model (DEM) data with higher precision for better and more detailed tsunami disaster modelling (Sarah, 2024).
2. Ensure inundation modelling is based on detailed topographic data, ideally with a vertical resolution of less than 0.25 m (Berryman, 2005).
3. Build upon the existing DEMNAS data, which has a resolution of 0.27 arc seconds, as it is superior to other freely available DEM data.
4. Consider using even higher-resolution data sources, such as photogrammetry and LiDAR, to improve modelling accuracy and detail.
5. The tourism management and local community around Sawarna Beach are advised to use tsunami inundation modelling results as a reference in infrastructure development and mitigation planning. For example, avoiding permanent construction in flood-prone areas and installing warning signs and evacuation instructions.

#### REFERENCES

- Adriano, B., Mas, E., Koshimura, S., & Gokon, H. 2020. Validation of Tsunami Numerical Model Using Observed Data of Building Damage and Flow Depth in the 2018 Sulawesi Tsunami. *Coastal Engineering Journal*, 62(1), 87–102. <https://doi.org/10.1080/21664250.2020.1723873>

- Badan Informasi Geospasial. 2025. Ina-Geoportal. Indonesia.go.id. <https://tanahair.indonesia.go.id/portal-web/unduh>
- Berryman, K. 2005. Review of Tsunami Hazard and Risk in New Zealand. <https://www.hbemergency.govt.nz/assets/Documents/Hazard-Reference-Documents/review-of-tsunami-hazard-and-risks-in-nz-sept-05.pdf>
- BNPB. 2012. Peraturan Kepala Badan Nasional Penanggulangan Bencana Nomor 02 Tahun 2012 tentang Pedoman Umum Pengkajian Risiko Bencana. <https://bpbd.natunakab.go.id/wp-content/uploads/2024/03/Peraturan-Kepala-BNPB-No-02-Tahun-2012.pdf>
- BNPB. 2023. Risiko Bencana Indonesia: Memahami Risiko Sistemik di Indonesia. Pusat Data, Informasi, dan Komunikasi Kebencanaan BNPB.
- Budiman, M. J., Sutoyo, & Syafiudin, M. F. 2024. Pemetaan Kerentanan Bahaya Tsunami dengan Pemodelan Inundasi (Studi Kasus: Kabupaten Bantul). *Jurnal Teknik Sipil Dan Lingkungan*, 9(2), 157–166. <https://doi.org/10.29244/jsil.9.2.157-166>
- Fitriani, L., Sutrisno, A., & Hidayat, R. 2024. Scenario-Based Tsunami Hazard Assessment Using Multi-Wave Simulations in Southern Banten. *Geoscience Frontiers*. <https://doi.org/10.1016/j.gsf.2024.101572>
- Goto, K., Chagué-Goff, C., Fujino, S., & Nishimura, Y. 2011. Inundation Distances and Flow Depths of Recent Tsunamis Inferred from Geological Data. *Earth-Science Reviews*, 107(1-2), 38–51. <https://doi.org/10.1016/j.earscirev.2011.03.002>
- Gusman, A. R., Tanioka, Y., & Latief, H. 2023. Influence of Topographic Roughness and Vegetation on Tsunami Wave Energy Dissipation Inland. *Journal of Geophysical Research: Oceans*, 128(2), e2022JC018926. <https://doi.org/10.1029/2022JC018926>
- Iswari, M. Y., & Anggraini, K. 2018. DEMNAS: Model Digital Ketinggian Nasional untuk Aplikasi Kepesisiran. *OSEANA*, 43(68), 68–80. <https://doi.org/10.14203/oseana.2018.Vol.43No.4.2>
- Koesoemadinata, R. P. 2020. An Introduction into the Geology of Indonesia (Vol. 1). Ikatan Alumni Teknik Geologi ITB.
- McCaffrey, R. 2008. Global Frequency of Magnitude 9 Earthquakes. *Geology*, 36(3), 263. <https://doi.org/10.1130/g24402a.1>
- Mori, N., Takahashi, T., Yasuda, T., & Yanagisawa, H. 2011. Survey of 2011 Tohoku Earthquake Tsunami Inundation and Run-Up. *Geophysical Research Letters*, 38(7). <https://doi.org/10.1029/2011GL049210>
- Prasetya, G. S., Imamura, F., & Gusman, A. R. 2021. High-Resolution Tsunami Inundation Modeling and Hazard Mapping for the Southern Coast of Java, Indonesia. *Natural Hazards*, 109(3), 2147–2169. <https://doi.org/10.1007/s11069-021-04934-3>
- Putra, A. A., Wibowo, H., & Hadi, S. 2022. Integrating DEMNAS and Land Use Data for Tsunami Risk Zoning in Pangandaran, Indonesia. *International Journal of Disaster Risk Reduction*, 72, 102845. <https://doi.org/10.1016/j.ijdr.2022.102845>
- Rahayu, H. P., Comfort, L. K., Khoirunnisa, D., & Nurhasanah, D. 2024. Need Assessment for Coastal Tourism Area in the Face of Tsunami Risk: The Case of Pangandaran. *International Journal on Advanced Science Engineering Information Technology*, 14(2), 563–574.

- Sarah, R., Awaluddin, M., & Hadi, F. 2024. Analisis Bahaya Tsunami di Kota Cilegon Menggunakan Sistem Informasi Geografis. *Jurnal Geodesi Universitas Diponegoro* Januari, 13(1), 58–64.
- Sundar, V., Sannasiraj, S. A., Murali, K., & Sriram, V. 2020. *Tsunami: Engineering Perspective for Mitigation, Protection and Modelling* (Vol. 50). World Scientific Publishing.  
<https://books.google.co.id/books?id=z3fpDwAAQBAJ>
- Suri, S. A., Sutoyo, & Syafiudin, M. F. 2024. Analisis Dampak Bencana Tsunami dan Perencanaan Jalur Evakuasi (Studi Kasus: Kabupaten Sukabumi). *Jurnal Teknik Sipil Dan Lingkungan*, 9(1), 11–20.  
<https://doi.org/10.29244/jsil.9.1.11-20>
- Tanioka, Y., Gusman, A. R., Satake, K., & Latief, H. 2018. Tsunami Scenario Simulations for the Java Subduction Zone Using New Seismic and Bathymetric Data. *Journal of Disaster Research*, 13(6), 1082–1091.  
<https://doi.org/10.20965/jdr.2018.p1082>
- Tonini, R., Di Manna, P., Lorito, S., Selva, J., Volpe, M., Romano, F., Basili, R., Brizuela, B., Castro, M. J., de la Asunción, M., Di Bucci, D., Dolce, M., Garcia, A., Gibbons, S. J., Glimsdal, S., González-Vida, J. M., Løvholt, F., Macías, J., Piatanesi, A., & Pizzimenti, L. 2021. Testing Tsunami Inundation Maps for Evacuation Planning in Italy. *Frontiers in Earth Science*, 9.  
<https://doi.org/10.3389/feart.2021.628061>
- USGS. 2019. Search Earthquake Catalog. [Usgs.gov.](https://earthquake.usgs.gov/earthquakes/search/)  
<https://earthquake.usgs.gov/earthquakes/search/>
- Wahyudi, A., Priadmodjo, A., Aksa, A., & Islaha, F. A. 2024. Pemetaan Skenario Genangan Tsunami Berbasis Pemodelan Spasial. *Jurnal Penelitian Pendidikan Geografi*, 9(1), 44–51.  
<http://creativecommons.org/licenses/by-nc/4.0>
- Wei, Y., Bernard, E. N., Titov, V., Moore, C., Spillane, M., Hopkins, M., & Mofjeld, H. 2013. Inundation Modeling and Mapping of Tsunami Hazards in the US Pacific Northwest. *Natural Hazards*, 65, 253–276. <https://doi.org/10.1007/s11069-012-0350-y>
- Yudhicara, Cipta, A., Maemunah, I., Lewu, A. P., & Nurfalalah, F. 2023. Katalog Tsunami Indonesia Tahun 416 - 2021 (A. Budianto, S. Hidayati, & Supartoyo, Eds.; pp. 52–65). Pusat Vulkanologi dan Mitigasi Bencana Geologi.

**APPENDIX**

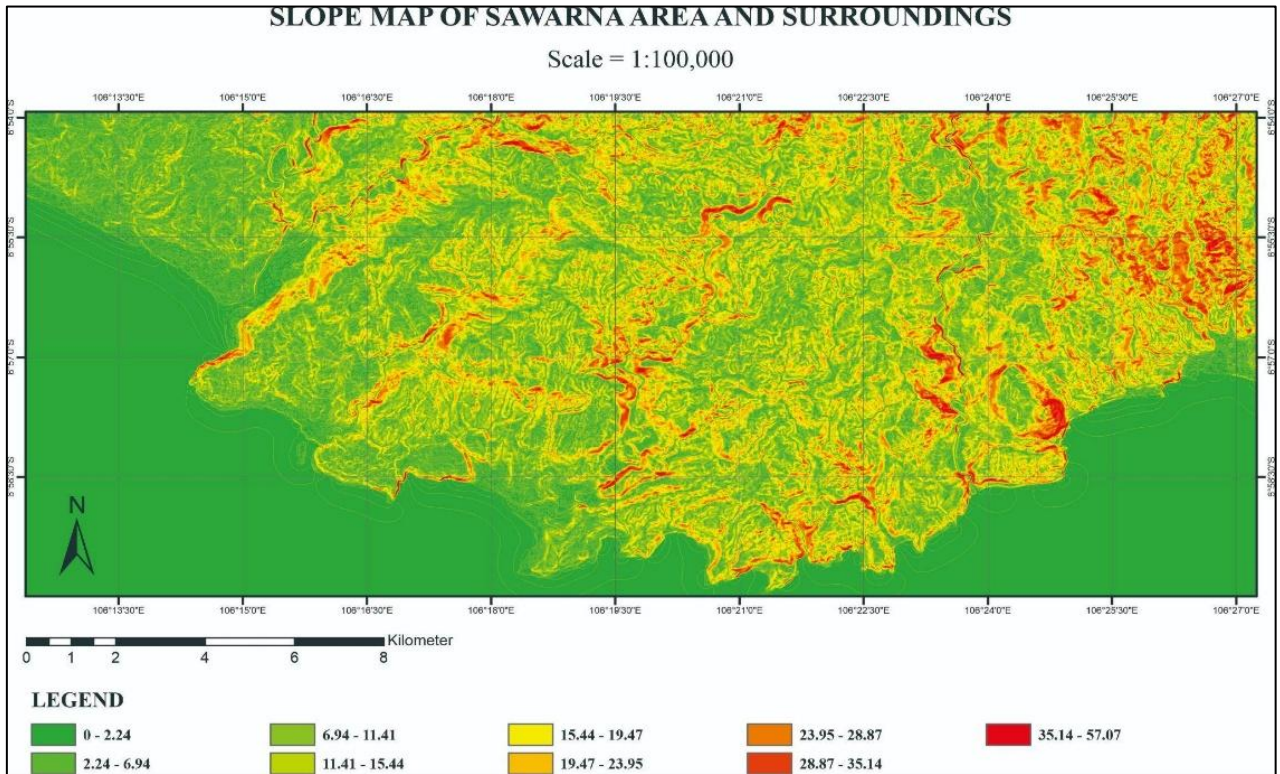


Fig. 4. The slope map of the Sawarna area shows that the western coast has gentle slopes ( $0^{\circ}$ – $6.94^{\circ}$ ), indicating flat terrain. In contrast, the eastern area has steeper slopes, mostly between  $15.44^{\circ}$  and  $28.87^{\circ}$ , especially in the hills (with the steepest areas  $35.14^{\circ}$ – $57.07^{\circ}$ ). Flatter areas are more likely to experience wider tsunami inundation.

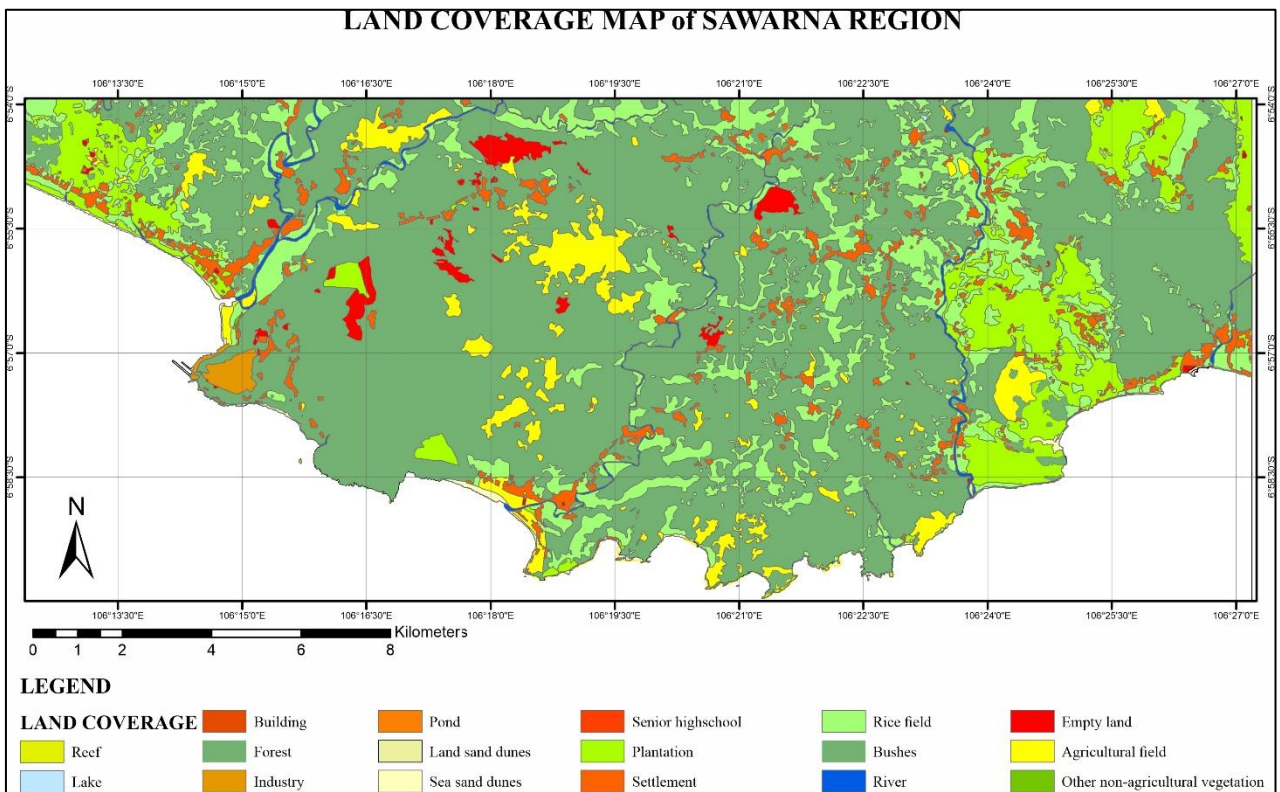


Fig. 3. Land Cover Map of Sawarna Area

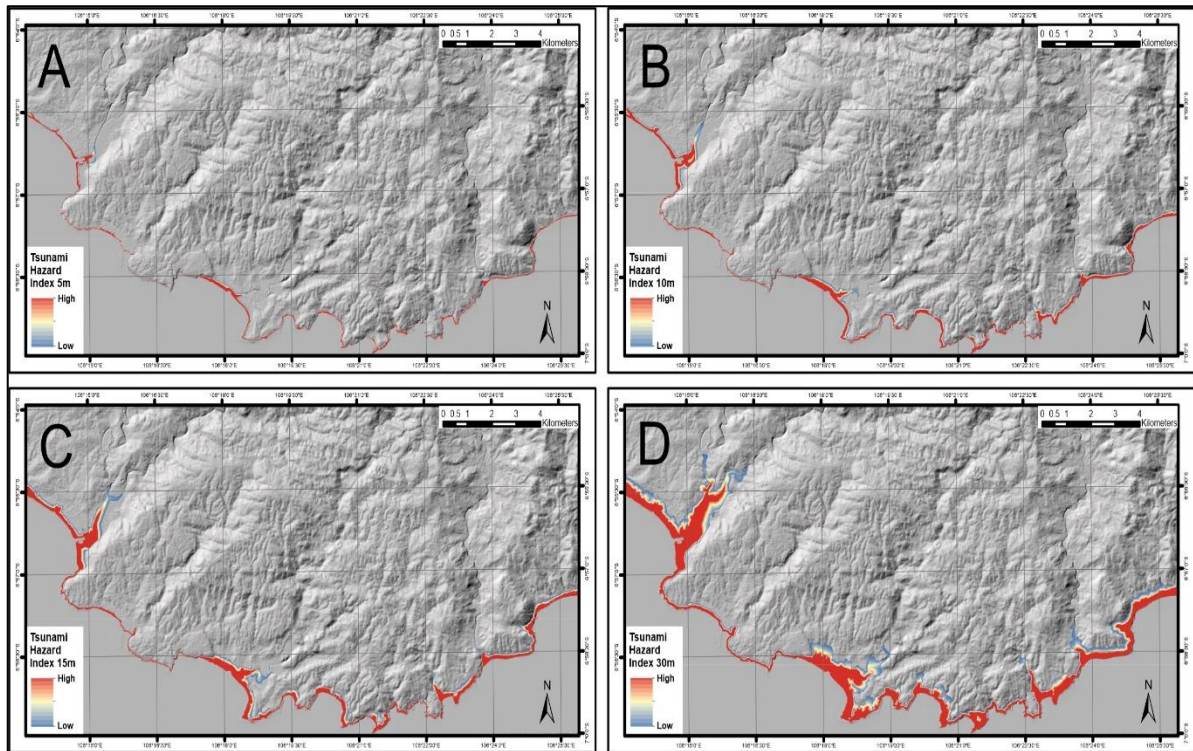


Fig. 5. The Tsunami Hazard Index shows the influence area of several Tsunami waves. Figure A is for 5m waves. Figure B is for 10m waves. Figure C is for 15m waves. Figure D is for 30m Tsunami waves.

